Supplementary information S1

Methods

Computational modeling

The following software packages were used on an Ubuntu 14.04 LTS system with either an Intel Xeon E3-1230 V2 with a GeForce GTX 660Ti or an Intel Core i7-5820K with a GeForce GTX 980: Chimera (Pettersen et al., 2004), Modeller (Webb and Sali, 2014), Swiss-PDB viewer Deepview (Guex et al., 2009), GROMACS 4.6.5 or 5.1.2 (Pronk et al., 2013), the AMBER99sb force field (Lindorff-Larsen et al., 2010), the Stockholm lipids forcefield (Jambeck and Lyubartsev, 2012), CUDA 7.5 (Nickolls et al., 2008) and ACPYPE (Sousa da Silva and Vranken, 2012) using *antechamber* from the AMBER 14 suite (Jambeck and Lyubartsev, 2014). The Lengau server at the Centre for High Performance Computing (CHPC, Cape Town, South Africa) was used for long-range simulations.

The Basic Local Alignment Search Tool (BLAST) was used to find solved GPCR protein structures in the Protein Data Bank (www.rcsb.org). All the structures with an E-value of less than $1x10^{-5}$ were chosen as potential templates. These include 4MQS (M2 muscarinic receptor) (Kruse et al., 2013), 4DAJ (M3 muscarinic receptor) (Kruse et al., 2012), 3PWH (adenosine A2A receptor) (Dore et al., 2011), 4BVN (β1-adrenergic receptor) (Miller-Gallacher et al., 2014), 3PBL (D3 dopamine receptor) (Chien et al., 2010), 3RZE (histamine H1 receptor) (Shimamura et al., 2011), 4N6H (δ-opioid receptor) (Fenalti et al., 2014), 4DKL (μ-opioid receptor) (Manglik et al., 2012), 3VW7 (protease-activated receptor 1) (Zhang et al., 2012), 2KS9 (NK1 neurokinin receptor), 4MBS (CCR5 chemokine receptor) (Tan et al., 2013), 2LNL (CXCR1 chemokine receptor) (Park et al., 2012), 3ODU (CXCR4 chemokine receptor) (B Wu et al., 2010), 1F88 (bovine rhodopsin) (Palczewski et al., 2000), 4S0V (OX2 orexin receptor) (Yin et al., 2015), 4GRV (NTSR1 neurotensin receptor) (White et al., 2012), 4EA3 (nociceptin/orphanin FQ receptor) (Thompson et al., 2012) and 4DJH (κ-opioid receptor) (H Wu et al., 2012). The GPCR database alignment tool (gpcrdb.org) was used to determine the TM, intracellular loop (ICL) and extracellular loop (ECL) domains of the receptors (Isberg et al., 2017). The MUltiple Sequence Comparison by Log-Expectation (MUSCLE) alignment tool (Edgar, 2004) was used to compare the sequences of TM1-ICL1-TM2, TM2-ECL1-TM3, TM3-ICL2-TM4, TM4-ECL2-TM5, TM5-ICL3-TM6 and TM6-ECL3-TM7 of the receptors to identify the optimal template structures for the ICL and ECL segments of the GnRH receptor. The NTSR1 neurotensin receptor was a good fit for TM1-ICL1-TM2, TM4-ECL2-TM5 and TM5-ICL3-TM5, whereas the OX2 orexin receptor was the best fit for TM2-ECL1-TM3 and TM3-ICL2-TM4 and the NK1 neurokinin receptor was the best fit for TM6-ECL3-TM7 (Supplementary information, Figures S1-S6). Modeller and Deepview Swiss-PDB viewer (Guex et al., 2009; Webb and Sali, 2014) were used to generate a homology model of the GnRH receptor using the 4GRV (NTSR1 neurotensin receptor) structure as a template for the TM helices and ECL2. ECL1 and ICL2 were modelled from the 4S0V (OX2 orexin receptor) crystal structure (Yin et al., 2015) by cutting the regions from positions 2.50 to 3.50 and 3.50 to 4.50, and superimposing them onto the 4GRV template using the match program in Chimera

(Pettersen et al., 2004). ECL3 from the 2KS9 NK1 neurokinin receptor template was used by cutting the region from positions 6.50 to 7.50 and superimposing it onto the 4GRV template. After superimposing the structures, the corresponding regions from the neurotensin structure 4GRV were removed. The final structure from this process was used as a template for homology modelling. Deepview Swiss-PDB viewer was used to ensure that disulphide bonds were formed between Cys^{14} in the amino terminal domain and Cys^{200} in ECL2 as described (Davidson et al., 1997) and between $Cys^{3.25(114)}$ and Cys^{196} in ECL2. The GnRH receptor homology model was superimposed on the 4GRV structure and its orientation in a lipid bilayer was determined using the OPM server (Lomize et al., 2012; Oda et al., 2005). The protein complex was placed in an 85x85 Angstrom 1-palmitoyl-2-oleoyl-sn-glycero-3-phosphoethanolamine (POPE) lipid membrane. Homology models of mutant receptors were generated by substituting Lys, Asp or Arg for $Glu^{2.53(90)}$ and Arg for $Trp^{6.48(280)}$.

Molecular dynamics simulations were performed on wild-type and mutant GnRH receptor homology models using GROMACS 4.6.5 (Pronk et al., 2013) and the AMBER99sb force field for proteins (Lindorff-Larsen et al., 2010). The non-bonded force calculations were accelerated through GPU acceleration using CUDA 7.5 (Nickolls et al., 2008). The complex was minimized with the steepest descent algorithm and the Verlet cut-off scheme. The system was prepared by heating it to 310 K (tau_t=0.2) during a 1 ns constant volume simulation with 2 fs time step using the modified Berendsen thermostat (V-rescale) using velocity rescaling (Berendsen et al., 1984; Bussi et al., 2007). The pressure was equilibrated to 1 atm during a 5 ns constant pressure simulation with a 2 fs time step using the Parrinello-Rahman parameters for pressure coupling (Nosé and Klein, 1983). In both simulations, all heavy atoms were position restrained with the force constant of 1000 kJ/(mol.nm^2). In the resulting models, interhelical contacts between amino acids are defined as a distance between any pair of atoms (side-chain and/or main-chain atoms) that is within the Euclidean distance (the sum of the van der Waal's radii of the atoms plus 0.6 Å) (Venkatakrishnan et al., 2013).

For the subsequent 100 ns molecular dynamics production runs the temperature and pressure were maintained at 310 K and 1 atm using the Berendsen thermostat (V-rescale) and Parrinello–Rahman pressure coupling method. The short-range non-bonded interactions were computed for the atom pairs within the cut-off of 1 nm and the long-range electrostatic interactions were calculated using particle-mesh-Ewald summation method with fourth-order cubic interpolation and 0.12 nm grid spacing (Darden et al., 1993). The parallel Linear Constraint Solver (LINCS) method was used to constrain bonds (Hess, 2008). 2000 snapshots over the 100 ns simulation were taken for analysis (every 25000 steps).

Results

Computational modeling

Modelling the wild-type GnRH receptor with a negatively-charged $Glu^{2.53(90)}$ side-chain resulted in deformation of the TM2 and TM3 helices, whereas a 75ns molecular dynamics simulation with a protonated $Glu^{2.53(90)}$ side-chain showed preserved helical structures of TM2

and TM3. Therefore, the uncharged (protonated) forms of the acidic amino acid side-chains were used in position 2.53(90) for the models of the wild-type and the Glu$^{2.53(90)}$Asp mutant receptors. The models exhibited all conformation-independent interhelical contacts that are conserved in the experimentally-determined (crystal) structures of both inactive and active class A GPCRs (Cvicek et al., 2016; Flanagan and Manilall, 2017; Venkatakrishnan et al., 2013), except for one (Supplementary table S1).

The wild-type GnRH receptor model showed that the Glu$^{2.53(90)}$ side-chain makes contact with the side-chain of Ser$^{3.35(124)}$ via van der Waals interactions (Fig. 3A, table 2) that were preserved during the molecular dynamics production run (Supplementary Fig. S7). The Glu$^{2.53(90)}$ side-chain also makes non-conserved direct interhelical contacts with the Trp$^{6.48(280)}$ residue of the CWxPY motif in TM6 and with the Phe$^{7.43(313)}$ and Pro$^{7.45(316)}$ residues in TM7 (Fig 3A, table 2), which were also preserved during molecular dynamics (Supplementary Fig. S8). However, Glu$^{2.53(90)}$ does not contact Lys$^{3.32(121)}$ (Fig. 3A) and during the molecular dynamics simulation Glu$^{2.53(90)}$ came close enough to Lys$^{3.32(121)}$ to form a salt-bridge for only 0.75% of the time (Supplementary Fig. S9).

The wild-type GnRH receptor model also showed the major intramolecular interactions characteristic of inactive GPCR structures, including the “closed” form of the core triad or transmission switch (Deupi, 2014; Deupi and Standfuss, 2011; Flanagan and Manilall, 2017; Huang et al., 2015; Trzaskowski et al., 2012), which was stable throughout the molecular dynamics simulation (Supplementary Fig. S10), and the Phe$^{1.53(56)}$-Tyr$^{7.53(323)}$ and Ile$^{3.46(135)}$-Thr$^{6.37(269)}$ interhelical contacts that define the inactive GPCR conformation, consistent with the absence of an agonist ligand (Flanagan and Manilall, 2017; Venkatakrishnan et al., 2016).

The starting model of the Glu$^{2.53(90)}$Lys mutant GnRH receptor showed a van der Waals interaction of the introduced Lys$^{2.53(90)}$ side-chain with Ser$^{3.35(124)}$ (Fig. 3B), similar to that in the wild-type GnRH receptor model, but it was broken during the molecular dynamics simulation (table 2, Supplementary Fig. S7), suggesting that it is unstable. The introduced Lys$^{2.53(90)}$ preserved interactions with Trp$^{6.48(280)}$ and Phe$^{7.43(313)}$, but the distance to Pro$^{7.46(316)}$ was more variable (table 2, Supplementary Fig. S8). The model of the Glu$^{2.53(90)}$Lys mutant receptor also showed the closed form of the core triad, but this opened during molecular dynamics (Supplementary Fig. S10), suggesting that the mutation has long-range destabilising effects on intramolecular contacts that stabilise the inactive receptor conformation.

The starting Glu$^{2.53(90)}$Asp mutant GnRH receptor model showed a preserved contact of Asp$^{2.53(90)}$ with Ser$^{3.35(124)}$ (Fig 3C) that did not change during the 100 ns molecular dynamics simulation (table 2, Supplementary Fig. S7C). However, there was no interaction with Trp$^{6.48(280)}$ (Fig 3C) and the Asp$^{2.53(90)}$ side-chain did not come close enough to Trp$^{6.48(280)}$ during molecular dynamics simulations to form a TM2-TM6 interhelical contact (table 2, Supplementary Fig. S8). Asp$^{2.53(90)}$ did form contacts with the TM7 residues Phe$^{7.43(313)}$ and Pro$^{7.46(316)}$ (Fig. 3C), but the contact with Phe$^{7.43(313)}$ was not preserved during molecular dynamics (table 2, Supplementary Fig. S8), suggesting that it is unstable due to the shorter length of the Asp side-chain. The starting model showed the closed form of the core triad, but the barrier opened during molecular dynamics (Supplementary Fig. S10) suggesting that the mutation indirectly destabilises intramolecular contacts that constitute the inactive receptor conformation.

The model of the $Glu^{2.53(90)}$Arg mutant GnRH receptor showed that the introduced $Arg^{2.53(90)}$ side-chain made interhelical contacts with $Ser^{3.35(124)}$ (Fig 3D) via van der Waals interactions that were similar to those in the wild-type receptor model and preserved during the molecular dynamics simulation (table 2, Supplementary Fig S7). The $Arg^{2.53(90)}$ side-chain made a direct contact with $Trp^{6.48(280)}$ of the CWxPY (Fig. 3D), which was preserved after the 100ns molecular dynamics run (table 2, Supplementary Fig. S8). Unlike the $Glu^{2.53(90)}$Lys and $Glu^{2.53(90)}$Asp mutants, the residues of the core triad did not diverge and the inactive receptor conformation remained stable (Supplementary Fig. S10).

In the simulation of the $Trp^{6.48(280)}$Arg mutant GnRH receptor interhelical contacts of $Glu^{2.53(90)}$ with $Ser^{3.35(124)}$ and $Pro^{7.46(316)}$ were preserved (table 2, Supplementary Figs. S7 and S8). The introduction of the Arg at position 6.48(280) resulted in a stable hydrogen bond being formed between $Arg^{6.48(280)}$ and $Glu^{2.53(90)}$ (table 2, Supplementary Fig. S8). The core triad and the inactive receptor conformation remained stable similar to the wild-type and $Glu^{2.53(90)}$Arg mutant (Supplementary Fig. S10).

To assess the effects of the side-chain lengths of amino acids substituted for $Glu^{2.53(90)}$ and $Trp^{6.48(280)}$ on the distances between TM2 and TM6, we measured the distances between the backbone carbons of the amino acids in the 2.53(90) and 6.48(280) loci (Fig. 4). The model of the wild-type receptor showed an average interhelical distance of 12.34 ± 0.017 Å from the backbone carbon atom, CA, of $Glu^{2.53(90)}$ to CA of $Trp^{6.48(280)}$. In the model of the $Glu^{2.53(90)}$Arg mutant receptor, the average distance between CA of $Arg^{2.53(90)}$ and CA of $Trp^{6.48(280)}$ was increased (14.33 ± 0.018 Å). The $Trp^{6.48(280)}$Arg mutant receptor also showed an increased average distance (13.11 ± 0.008) between CA of $Arg^{6.48(280)}$ and $Glu^{2.53(90)}$. The stability of this interaction (Fig. 4) is most likely due to a stable hydrogen bond between the $Arg^{6.48(280)}$ and $Glu^{2.53(90)}$ side-chains.

A

```
CLUSTAL multiple sequence alignment by MUSCLE (3.8)

GnRH1_receptor          ---------KIRVTVTFFLFLLSATFNASFLLKLQKWTQKKEKGKKLSRMKLLLKHLTLA
Rhodopsin               -------PWQFSMLAAYMFLLIVLGFPINFLTLYVTVQHKKLR----TPLNYILLNLAVA
PAR1                    -------SWLTLFVPSVYTGVFVVSLPLNIMAIVVFILKMKVK----KPAVVYMLHLATA
M2_receptor             ------KTFEVVFIVLVAGSLSLVTIIGNILVMVSIKVNRHLQ----TVNNYFLFSLACA
M3_receptor             -------VWQVVFIAFLTGILALVTIIGNILVIVSFKVNKQLK----TVNNYFLLSLACA
NTS1_receptor           -------IYSKVLVTAVYLALFVVGTVGNTVTAFTLARKKSLQSLQ-STVHYHLGSLALS
H1_receptor             ------------PLVVVLSTICLVTVGLNLLVLYAVRSERKLH----TVGNLYIVSLSVA
beta1-adrenoceptor      ---EPLSQQWTAGMGLLMALIVLLIVAGNVLVIVAIAKTPRLQ----TLTNLFIMSLASA
A2A-adrenoceptor        -------LQVTLTLVCLAGLLMLLTVFGNVLVIIAVFTSRALK----APQNLFLVSLASA
D3_receptor             -------ARPHAYYALSYCALILAIVFGNGLVCMAVLKERALQ----TTTNYLVVSLAVA
CXCR1                   -----TETLNKYVVIIAYALVFLLSLLGNSLVMLVILYSRVGR----SVTDVYLLNLALA
CXCR4                   --REENANFNKIFLPTIYSIIFLTGIVGNGLVILVMGYQKKLR----SMTDKYRLHLSVA
CCR5                    --KINVKQIAARLLPPLYSLVFIFGFVGNMLVILILINCKRLK----SMTDIYLLNLAIS
NK1_receptor            ---------QIVLWAAAYTVIVVTSVVGNVVVMWIILAHKRMR----TVTNYFLVNLAFA
OX1_receptor            ----------EWVLIAAYVAVFVVALVGNTLVCLAVWRNHHMR----TVTNYFIVNLSLA
OX2_receptor            ----------YEWVLIAGYIIVFVVALIGNVLVCVAVWKNHHMR----TVTNYFIVNLSLA
delta_receptor          GARSASSLALAIAITALYSAVCAVGLLGNVLVMFGIVRYTKMK----TATNIYIFNLALA
mu_receptor             -------MITAITIMALYSIVCVVGLFGNFLVMYVIVRYTKMK----TATNIYIFNLALA
                                          :       . :           .            *: :

GnRH1_receptor          NLLETLIVMPLDGMWNI-
Rhodopsin               DLFMVLGGFTSTLYTSLH
PAR1                    DVLFVSV-LPFKISYYFS
M2_receptor             DLIIGVFSMNLYTLYTVI
M3_receptor             DLIIGVISMNLFTTYIIM
NTS1_receptor           DLLTLLLAMPVELYNFIW
H1_receptor             DLIVGAVVMPMNILYLLM
beta1-adrenoceptor      DLVMGLLVVPFGATIVVW
A2A-adrenoceptor        DILVATLVIPFSLANEVM
D3_receptor             DLLVATLVMPWVVYLEVT
CXCR1                   DLLFALT-LPIWAASKVN
CXCR4                   DLLFVIT-LPFWAVDAVA
CCR5                    DLFFLLT-VPFWAHYAAA
NK1_receptor            EASMAAFNTVVNFTYAV-
OX1_receptor            DVLVTAICLPASLLVDIT
OX2_receptor            DVLVTIITCLPATLVVDIT
delta_receptor          DALATST-LPFQSAKYLM
mu_receptor             DALATST-LPFQSVNYLM
                        :
```

B

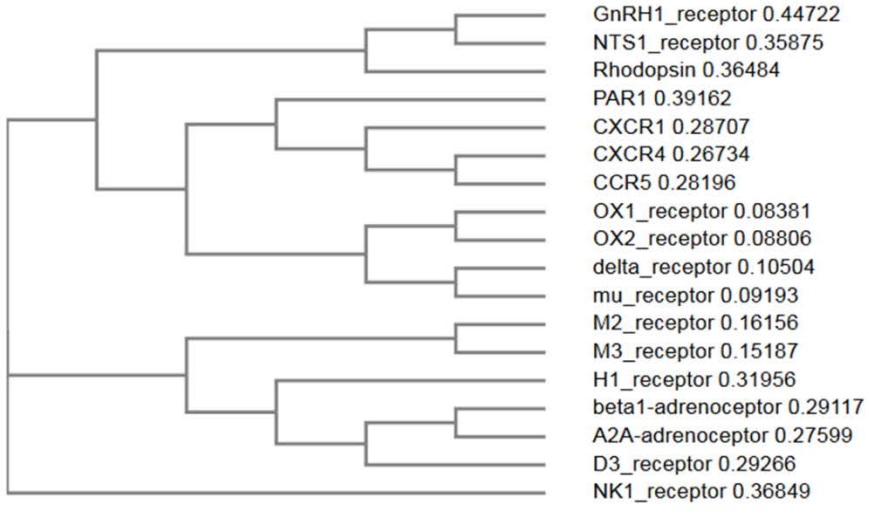

Figure S1: Alignment (A) and phylogenetic analysis (B) of TM1-ICL1-TM2.

A

```
CLUSTAL multiple sequence alignment by MUSCLE (3.8)


Rhodopsin               TPLNYILLNLAVADLFMVLGGFTSTLYTSL--HGYFVFGPTGCNLEGFFATLGGEIALWS
NK1_receptor            TVTNYFLVNLAFAEASMAAFNTVVNFTYAV--HNEWYYGLFYCKFHNFFPIAAVFASIYS
beta1-adrenoceptor      TLTNLFIMSLASADLVMGLLVVPFGATIVV--WGRWEYGSFFCELWTSVDVLCVTASIET
A2A-adrenoceptor        APQNLFLVSLASADILVATLVIPFSLANEV-M-GYWYFGKAWCEIYLALDVLFCTSSIVH
D3_receptor             TTTNYLVVSLAVADLLVATLVMPWVVYLEV-TGGVWNFSRICCDVFVTLDVMMCTASILN
M2_receptor             TVNNYFLFSLACADLIIGVFSMNLYTLYTV--IGYWPLGPVVCDLWLALDYVVSNASVMN
M3_receptor             TVNNYFLLSLACADLIIGVISMNLFTTYII-MNR-WALGNLACDLWLAIDYVASNASVMN
H1_receptor             TVGNLYIVSLSVADLIVGAVVMPMNILYLL-MSK-WSLGRPLCLFWLSMDYVASTASIFS
NTS1_receptor           STVHYHLGSLALSDLLTLLLAMPVELYNFIWVHHPWAFGDAGCRGYYFLRDACTYATALN
GnRH1_receptor          -RMKLLLKHLTLANLLETLIVMPLDGMWNI-TVQ-WYAGELLCKVLSYLKLFSMYAPAFM
OX1_receptor            TVTNYFIVNLSLADVLVTAICLPASLLVDI-TES-WLFGHALCKVIPYLQAVSVSVAVLT
OX2_receptor            TVTNYFIVNLSLADVLVTITCLPATLVVDI-TET-WFFGQSLCKVIPYLQTVSVSVSVLT
PAR1                    KPAVVYMLHLATADVLF-VSVLPFKISYYF-SGSDWQFGSELCRFVTAAFYCNMYASILL
delta_receptor          TATNIYIFNLALADALA-TSTLPFQSAKYL-MET-WPFGELLCKAVLSIDYYNMFTSIFT
mu_receptor             TATNIYIFNLALADALA-TSTLPFQSVNYL-MGT-WPFGTILCKIVISIDYYNMFTSIFT
CCR5                    SMTDIYLLNLAISDLFF-LLTVPFWAHYAA---AQWDFGNTMCQLLTGLYFIGFFSGIFF
CXCR4                   SMTDKYRLHLSVADLLF-VITLPFWAVDAV---ANWYFGNFLCKAVHVIYTVNLYSSVLI
CXCR1                   SVTDVYLLNLALADLLF-ALTLPIWAASKV---NGWIFGTFLCKVVSLLKEVNFYSGILL
                                *: ::                     :  .   *

Rhodopsin               LVVLAIERYVVVCK
NK1_receptor            MTAVAFDRYMAIIH
beta1-adrenoceptor      LCVIALDRYLAITS
A2A-adrenoceptor        LCAISLDRYWSITQ
D3_receptor             LCAISIDRYTAVVM
M2_receptor             LLIISFDRYFCVTK
M3_receptor             LLVISFDRYFSITR
H1_receptor             VFILCIDRYRSVQQ
NTS1_receptor           VASLSVERYLAICH
GnRH1_receptor          MVVISLDRSLAITR
OX1_receptor            LSFIALDRWYAICH
OX2_receptor            LSCIALDRWYAICH
PAR1                    MTVISIDRFLAVVY
delta_receptor          LTMMSVDRYIAVCH
mu_receptor             LCTMSVDRYIAVCH
CCR5                    IILLTIDRYLAVVH
CXCR4                   LAFISLDRYLAIVH
CXCR1                   LACISVDRYLAIVH
                        :  : .:*   :
```

B

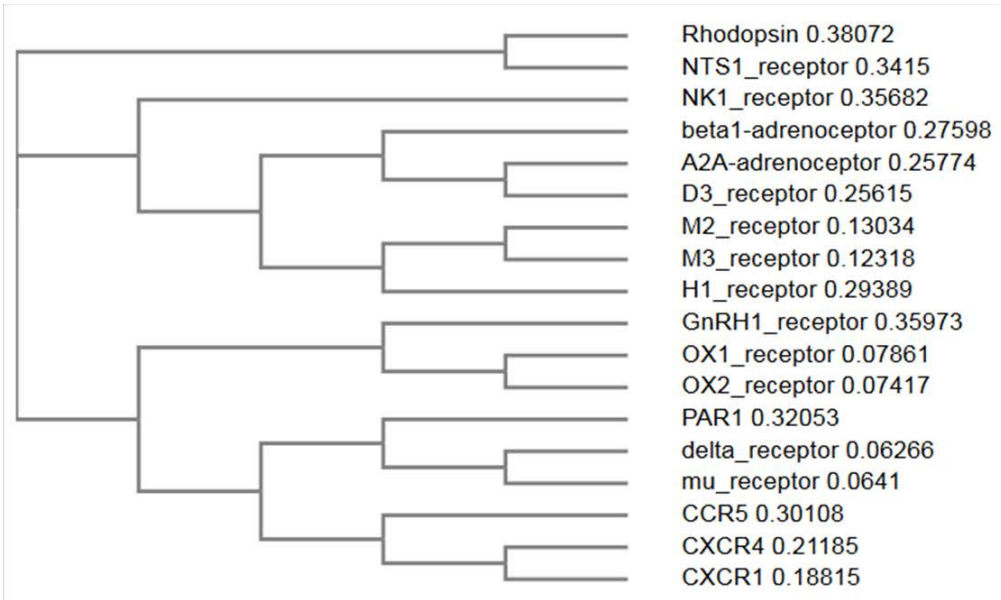

Figure S2: Alignment (A) and phylogenetic analysis (B) of TM2-ECL1-TM3.

A

```
CLUSTAL multiple sequence alignment by MUSCLE (3.8)


Rhodopsin               YFVFGPTGCNLEGFFATLGGEIALWSLVVLAIERYVVVCKPMSNFR---FGENHAIMGVA
NTS1_receptor           PWAFGDAGCRGYYFLRDACTYATALNVASLSVERYLAICHPFKAKT---LMSRSRTKKFI
CCR5                    QWDFGNTMCQLLTGLYFIGFFSGIFFIILLTIDRYLAVVHAVFALK---ARTVTFGVVTS
GnRH1_receptor          QWYAGELLCKVLSYLKLFSMYAPAFMMVVISLDRSLAITRPLALKS-----NSKVGQSMV
OX1_receptor            SWLFGHALCKVIPYLQAVSVSVAVLTLSFIALDRWYAICHPLLFKS-----TARRARGSI
OX2_receptor            TWFFGQSLCKVIPYLQTVSVSVSVLTLSCIALDRWYAICHPLMFKS-----TAKRARNSI
delta_receptor          TWPFGELLCKAVLSIDYYNMFTSIFTLTMMSVDRYIAVCHPVKALD---FRTPAKAKLIN
mu_receptor             TWPFGTILCKIVISIDYYNMFTSIFTLCTMSVDRYIAVCHPVKALD---FRTPRNAKIIN
PAR1                    DWQFGSELCRFVTAAFYCNMYASILLMTVISIDRFLAVVYPMQSLS---WRTLGRASFTC
M2_receptor             YWPLGPVVCDLWLALDYVVSNASVMNLLIISFDRYFCVTKPLTYPV---KRTTKMAGMMI
M3_receptor             RWALGNLACDLWLAIDYVASNASVMNLLVISFDRYFSITRPLTYRA---KRTTKRAGVMI
H1_receptor             KWSLGRPLCLFWLSMDYVASTASIFSVFILCIDRYRSVQQPLRYLK---YRTKTRASATI
D3_receptor             VWNFSRICCDVFVTLDVMMCTASILNLCAISIDRYTAVVMPVHYQHGTGQSSCRRVALMI
beta1-adrenoceptor      RWEYGSFFCELWTSVDVLCVTASIETLCVIALDRYLAITSPFRYQS---LLTRARARGLV
A2A-adrenoceptor        YWYFGKAWCEIYLALDVLFCTSSIVHLCAISLDRYWSITQAIEYNL---KRTPRRIKAII
NK1_receptor            EWYYGLFYCKFHNFFPIAAVFASIYSMTAVAFDRYMAIIHPLQPRL-----SATATKVVI
CXCR1                   GWIFGTFLCKVVSLLKEVNFYSGILLLACISVDRYLAIVHATRTLT----QKRHLVKFVC
CXCR4                   NWYFGNFLCKAVHVIYTVNLYSSVLILAFISLDRYLAIVHATNSQR---PRKLLAEKVVY
                         :  .   *                :  : .:*   :  .

Rhodopsin               FT-WVMALACAAPPLA-------
NTS1_receptor           SAIWLASALLAVPMLFTM-----
CCR5                    VITWVVAVFASLPGIIFT-----
GnRH1_receptor          GLAWILSSVFAGPQLYIF-----
OX1_receptor            LGIWAVSLAIMVPQAAVM-----
OX2_receptor            VIIWIVSCIIMIPQAIVM-----
delta_receptor          ICIWVLASGVGVPIMVMA-----
mu_receptor             VCNWILSSAIGLPVMFMA-----
PAR1                    LAIWALAIAGVVPLLLK------
M2_receptor             AAAWVLSFILWAPAILFWQFIVG
M3_receptor             GLAWVISFVLWAPAILFWQYFVG
H1_receptor             LGAWFLSF-LWVIPILG------
D3_receptor             TAVWVLAFAVSCPLLFG------
beta1-adrenoceptor      CTVWAISALVSFLPILMH-----
A2A-adrenoceptor        ITVWVISAVISFPPLIS------
NK1_receptor            CVIWVLALLLAFPQGYYS-----
CXCR1                   LGCWGLSMNLSLPFFLFR-----
CXCR4                   VGVWIPALLLTIPDFIFA-----
                           *  :
```

B

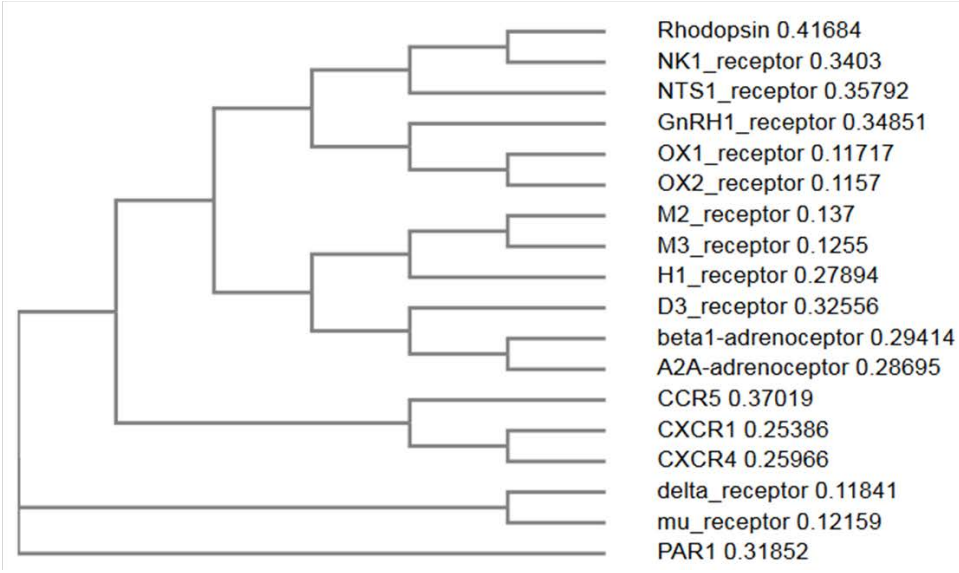

Figure S3: Alignment (A) and phylogenetic analysis (B) of TM3-ICL2-TM4.

A

```
CLUSTAL multiple sequence alignment by MUSCLE (3.8)


CXCR1                   KRHLVKFVCLGCWGLSMNLSLPFFLFRQAYHPNNSSP-----------VCYEVLGN-DTA
GnRH1_receptor          NSKVGQSMVGLAWILSSVFAGPQLYIFRMIHLADSSGQTKVFSQCVTHCSFSQWWH----
H1_receptor             TKTRASATILGAWFLSFLWVIPILGWNHFMQQTSVRRED---------KCETDFYD----
CCR5                    TVTFGVVTSVITWVVAVFASLPGI----IFTRSQKEGLHY--------TCSSHFPYSQYQ
NTS1_receptor           SRSRTKKFISAIWLASALLAVPML--FTMGEQNRSADGQHAGGL----VCTPTIHT---A
M2_receptor             TTKMAGMMIAAAWVLSFILWAPAILFWQFIVGVRTVEDG---------ECYIQFFS----
M3_receptor             TTKRAGVMIGLAWVISFVLWAPAILFWQYFVGKRTVPPG---------ECFIQFLS----
delta_receptor          TPAKAKLINICIWVLASGVGVPIM----VMAVTRPRDGAV--------VCMLQFPS-PSW
mu_receptor             TPRNAKIINVCNWILSSAIGLPVM----FMATTKYRQGSI--------DCTLTFSH-PTW
CXCR4                   KLLAEKVVYVGVWIPALLLTIPDF----IFANVSEADDRY--------ICDRFYPN---D
NK1_receptor            SATATKVVICVIWVLALLLAFPQG----YYSTTETMPSRV--------VCMIEWPEHPNK
PAR1                    TLGRASFTCLAIWALAIAGVVPLL----LKEQTIQVPGLNIT------TCHDVLNETLLE
OX1_receptor            TARRARGSILGIWAVSLAIMVPQA----AVMECSSVLPELANRTRLFSVCDERWAD---D
OX2_receptor            TAKRARNSIVIIWIVSCIIMIPQA----IVMECSTVFPGLANKTTLFTVCDERWGG---E
Rhodopsin               GENHAIMGVAFTWVMALACAAPPLAGW-----SRYIPEGLQC------SCGIDYYTLKPE
beta1-adrenoceptor      TRARARGLVCTVWAISALVSFLPILMHWWRAESDEARRCYNDPK----CCDFVTNR----
D3_receptor             SCRRVALMITAVWVLAFAVSCPLL----FGFNTTGDPT----------VCSISNPD----
A2A-adrenoceptor        TPRRIKAIIITVWVISAVISFPPL----ISIEKKGGGGGPQPAEP---RCEINDQK----
                                  *  :                                  .

CXCR1                   KWRMVLRILPHTFGFIVPLFVMLFCYGFTLRTLFKA--------
GnRH1_receptor          --QAFYNFFTFSCLFIIPLFIMLICNAKIIFTLTRVLHQDPH--
H1_receptor             --VTWFKVMTAIINFYLPTLLMLWFYAKIYKAVRQHCQHRELIN
CCR5                    FWKNFQTLKIVILGLVLPLLVMVICYSGILKTLLRC--------
NTS1_receptor           TVKVVIQVNTFM-SFIFPMVVISVLNTIIANKLTVMVRQAAEQG
M2_receptor             --NAAVTFGTAIAAFYLPVIIMTVLYWHISRASKSRIKKDKKE-
M3_receptor             --EPTITFGTAIAAFYMPVTIMTILYWRIYKETEKRTKELAGL-
delta_receptor          YWDTVTKICVFLFAFVVPILIITVCYGLMLLRLRSV--------
mu_receptor             YWENLLKICVFIFAFIMPVLIITVCYGLMILRLKSV--------
CXCR4                   LWVVVFQFQHIMVGLILPGIVILSCYCIIISKLSHS--------
NK1_receptor            IYEKVYHICVTVLIYFLPLLVIGYAYTVVGITLWASEIPGD---
PAR1                    GYYAYYFSAFSAVFFFVPLIISTVCYVSIIRCLSS---------
OX1_receptor            LYPKIYHSCFFIVTYLAPLGLMAMAYFQIFRKLWGRQIP-----
OX2_receptor            IYPKMYHICFFLVTYMAPLCLMVLAYLQIFRKLWCRQIP-----
Rhodopsin               VNNESFVIYMFVVHFTIPMIIIFFCYGQLVFTVKEAAAQQ----
beta1-adrenoceptor      ----AYAIASSVVSFYVPLCIMAFVYLRVFREAQKQVKKIDS--
D3_receptor             -----FVIYSSVVSFYLPFGVTVLVYARIYVVLKQRRRKRILTR
A2A-adrenoceptor        ----WYVISSCIGSFFAPCLIMILVYVRIYQIAKRRTRVPPSR-
                                  *  :
```

B

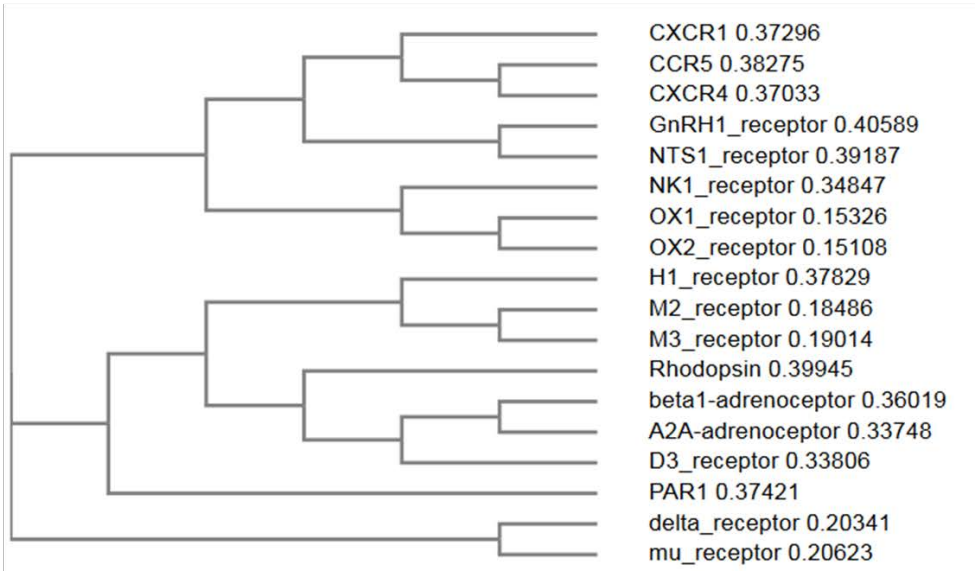

Figure S4: Alignment (A) and phylogenetic analysis (B) of TM4-ECL2-TM5.

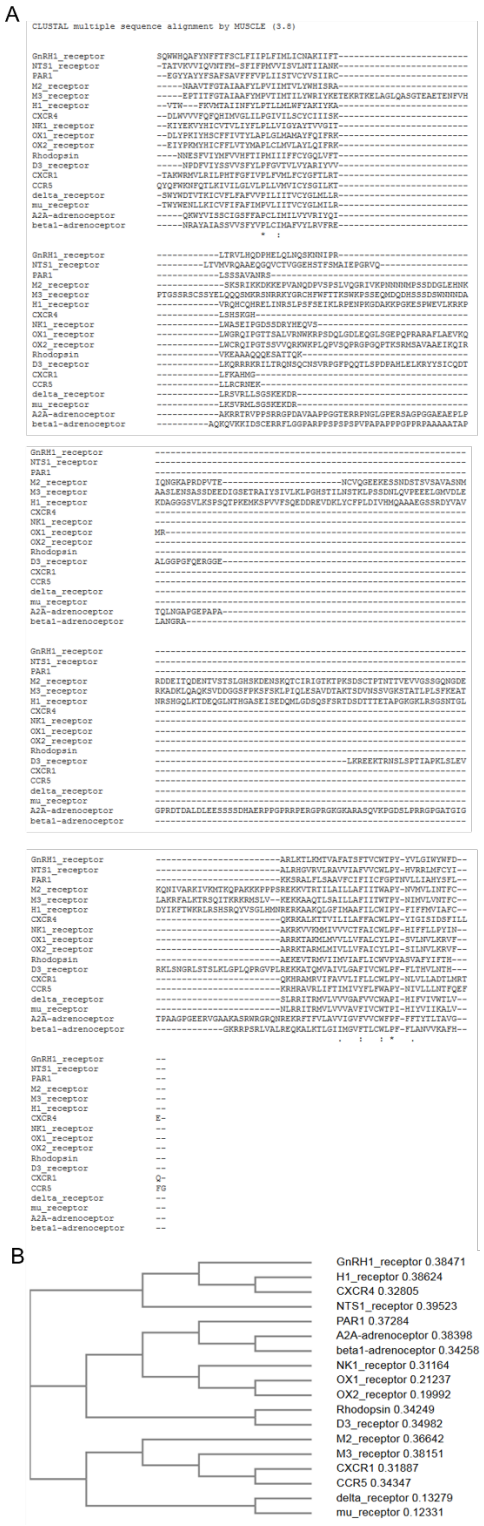

Figure S5: Alignment (A) and phylogenetic analysis (B) of TM5-ICL3-TM6.

A

```
CLUSTAL multiple sequence alignment by MUSCLE (3.8)

PAR1                    NRSKK------SRALFLSAAVFCIFIICFGPTNVLLIAH--YSFLSHTST---TEAAYFA
GnRH1_receptor          QSKNNIPRAR-LKTLKMTVAFATSFTVCWTPYYVLGIWY------WFDPE-MLNRLSDPV
Rhodopsin               ATTQKAE----KEVTRMVIIMVIAFLICWVPYASVAFYI------FTHQG---SNFGPIF
CXCR4                   K----------RKALKTTVILILAFFACWLPYYIGISIDSFILLEIIKQG---CEFENTV
CCR5                    KKR--------HRAVRLIFTIMIVYFLFWAPYNIVLLLNTFQEFFGLNN----CSSSNRL
CXCR1                   K----------HRAMRVIFAVVLIFLLCWLPYNLVLLADTLMRTQVIQES---CERRNNI
NK1_receptor            RYHEQVSAK--RKVVKMMIVVVCTFAICWLPFHIFFLLP------YINPDLYLKKFIQQV
NTS1_receptor           PGRVQAL----RHGVRVLRAVVIAFVVCWLPYHVRRLMF------CYISD---EQWTPFL
delta_receptor          SKEKDRSL---RRITRMVLVVVGAFVVCWAPIHIFVIVW---TLVDIDRR---DPLVVAA
mu_receptor             SKEKDRNL---RRITRMVLVVVAVFIVCWTPIHIYVIIK----ALVTIPE---TTFQTVS
OX1_receptor            FLAEVKQMRARRKTAKMLMVVLLVFALCYLPISVLNVLKRVFGMFRQASD---REAVYAC
OX2_receptor            VAAEIKQIRARRKTARMLMIVLLVFAICYLPISILNVLKRVFGMFAHTED---RETVYAW
A2A-adrenoceptor        RGRQNRE----KRFTFVLAVVIGVFVVCWFPFFFTYTLT--------AVG---CSVPRTL
D3_receptor             RGVPLRE----KKATQMVAIVLGAFIVCWLPFFLTHVLN------THCQT---CHVSPEL
beta1-adrenoceptor      RLVALRE----QKALKTLGIIMGVFTLCWLPFFLANVVK------AFHRE---L-VPDRL
H1_receptor             GLHMNRE----RKAAKQLGFIMAAFILCWIPYFIFFMVI------AFCKN---C-CNEHL
M2_receptor             KPPPSRE----KKVTRTILAILLAFIITWAPYNVMVLIN------TFCAP---C-IPNTV
M3_receptor             RMSLVKE----KKAAQTLSAILLAFIITWTPYNIMVLVN------TFCDS---C-IPKTF
                                              .   :   : *

PAR1                    YLLCVC-------VSSISCCIDPLIYYYAS
GnRH1_receptor          NHFFFL-------FAFLNPCFDPLIYGYF-
Rhodopsin               MTIPAF-------FAKSAAIYNPVIYIMMN
CXCR4                   HKWISI----TEALAFFHCCLNPILYAFLG
CCR5                    DQAMQV----TETLGMTHCCINPIIYAFVG
CXCR1                   GRALDA----TEILGFLHSCLNPIIYAFIG
NK1_receptor            YLAIMW-------LAMSSTMYNPIIYCCLN
NTS1_receptor           YDFYHYFYMVTNALFYVSSTINPILYNLVS
delta_receptor          LHLCIA-------LGYANSSLNPVLYAFLD
mu_receptor             WHFCIA-------LGYTNSCLNPVLYAFLD
OX1_receptor            FTFSHW-------LVYANSAANPIIYNFLS
OX2_receptor            FTFSHW-------LVYANSAANPIIYNFLS
A2A-adrenoceptor        FKFFFW-------FGYCNSSLNPVIYTIFN
D3_receptor             YSATTW-------LGYVNSALNPVIYTTFN
beta1-adrenoceptor      FVFFNW-------LGYANSAFNPIIYCRS-
H1_receptor             HMFTIW-------LGYINSTLNPLIYPLCN
M2_receptor             WTIGYW-------LCYINSTINPACYALCN
M3_receptor             WNLGYW-------LCYINSTVNPVCYALCN
                                     .       :*  *
```

B

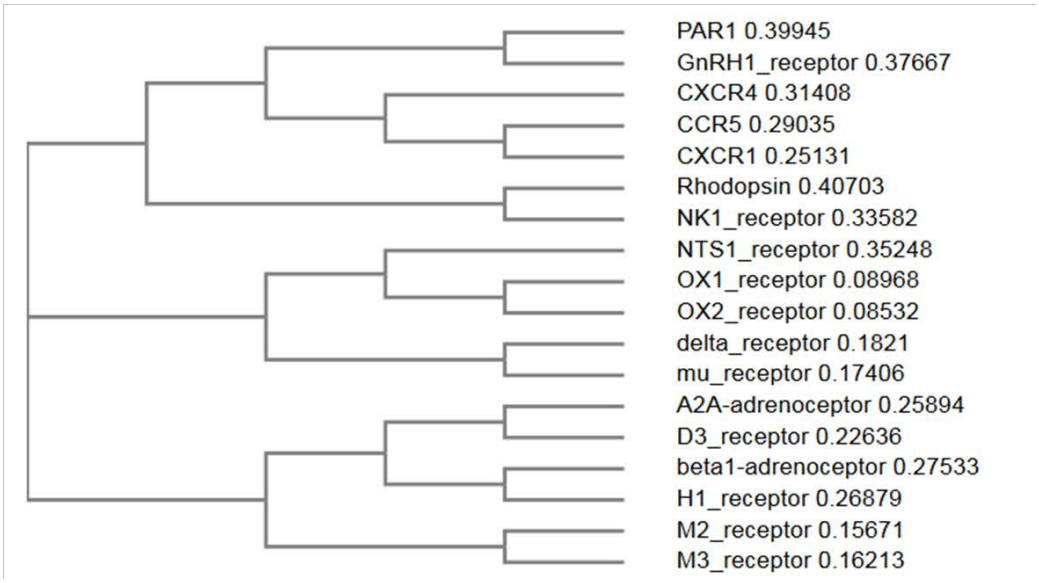

Figure S6: Alignment (A) and phylogenetic analysis (B) of TM6-ECL3-TM7.

Supplementary Table S1: Distance between conserved conformation-independent interhelical contacts (Cvicek et al., 2016; Flanagan and Manilall, 2017; Venkatakrishnan et al., 2013). Euclidian distance is defined as the distance between any pair of atoms (side-chain and/or main-chain atoms) that are within the sum of the van der Waal radii of the atoms plus 0.6 Å (van der Waal interaction distance) (Venkatakrishnan et al., 2013). CHH-associated mutations that affect conformation-independent interhelical contacts are also listed.

Amino acid A interaction with Amino acid B	Atom A	Atom B	Distance (Å)	cHH-associated mutations
F1.43-T2.54	CD1	OG1	3.627	
F1.43-M2.58	CA	CB	3.711	
S1.46-T2.54	CB	CB	3.772	
S1.46-C7.47	CB	CB	3.899	
F1.49-P7.50	CB	CB	3.774	$Pro^{(7.50)320}Leu$
N1.50-T2.47	OD1	HA	3.248	
N1.50-N2.50	OD1	ND2	3.071	
N1.50-L2.51	CB	CD2	3.431	
N1.50-P7.46	HD22	O	2.161	
N1.50-P7.50	OD1	CG	3.585	$Pro^{(7.50)320}Leu$
F1.53-T2.47	HB1	HG21	2.749	
L1.54-T2.47	CD2	CD	3.578	
L1.57-K2.44	HD22	HD1	2.985	
L2.42-V3.45	CD2	CG2	3.610	
L2.42-I3.46	HD21	HD2	2.746	$Val^{(3.45)134}Gly$
L2.43-Y7.53	HD23	OH	3.122	$Tyr^{(7.53)323}Cys$
H2.45-M3.42	HD2	N	3.163	$Met^{(3.42)131}Thr$
H2.45-M3.43	HD2	N	5.714	
H2.45-V4.46	CB	CG1	3.957	
L2.46-P3.39	HD21	HB2	2.498	
L2.46-M3.42	CB	CE	3.953	$Met^{(3.42)131}Thr$
N2.50-P7.46	OD1	HA	2.944	
E2.53-S3.35	CB	CB	3.848	$Glu^{(2.53)90}Asp$, $Glu^{(2.53)90}Lys$
F3.34-S4.53	CE1	CB	3.535	
F3.34-A4.57	CE2	CB	3.413	$Ala^{(4.57)171}Thr$
M3.36-W6.48	CG	CZ3	3.765	
M3.36-R6.48	HE3	HE3	3.157	
Y3.37-S4.53	CB	OG	3.832	
A3.38-W4.50	CB	CZ3	3.814	
A3.38-S4.53	HB3	HG	3.461	
A3.40-F6.44	CB	CZ	3.931	$Ala^{(3.40)129}Asp$
F3.41-A4.49	HD2	HB1	2.680	$Ala^{(4.49)163}Ser$
M3.43-F6.44	CE	CD2	3.367	
V3.44-M5.54	CG2	CG	3.903	
S3.47-C5.57	O	HB1	2.705	
S3.51-C5.57	OG	HG	2.109	

S3.51-K5.60	HG	HE2	2.752	
S3.51-I5.61	HA	HG21	2.825	
F5.47-Y6.52	CD1	CB	3.749	$Tyr^{(6.52)284}Cys$
M5.54-A6.41	HE1	HB3	2.542	
C6.47-F7.41	HA	HE1	2.746	$Cys^{6.47(279)}Tyr$
C6.47-A7.42	HB1	HA	2.349	$Cys^{6.47(279)}Tyr$
C6.47-N7.45	SG	CB	3.861	$Cys^{6.47(279)}Tyr$
W6.48-A7.42	CZ3	HB2	3.432	
R6.48-A7.42	NH1	HB1	2.683	
Y6.51-F7.38	CD1	CD2	3.948	$Tyr^{(6.51)283}His$
Y6.51-F7.39	CE2	CE2	3.934	$Tyr^{(6.51)283}His$

Supplementary Table S2: Van der Waals distance of each atom (Å).

Hydrogen	1.2
Carbon	1.7
Nitrogen	1.55
Oxygen	1.52
Sulfur	1.8

Supplementary Table S3: Euclidian distance matrix (Å).

	H	C	N	O	S
H	3	3.5	3.35	3.32	3.6
C	3.5	4	3.85	3.82	4.1
N	3.35	3.85	3.7	3.67	3.95
O	3.32	3.82	3.67	3.64	3.92
S	3.6	4.1	3.95	3.92	4.2

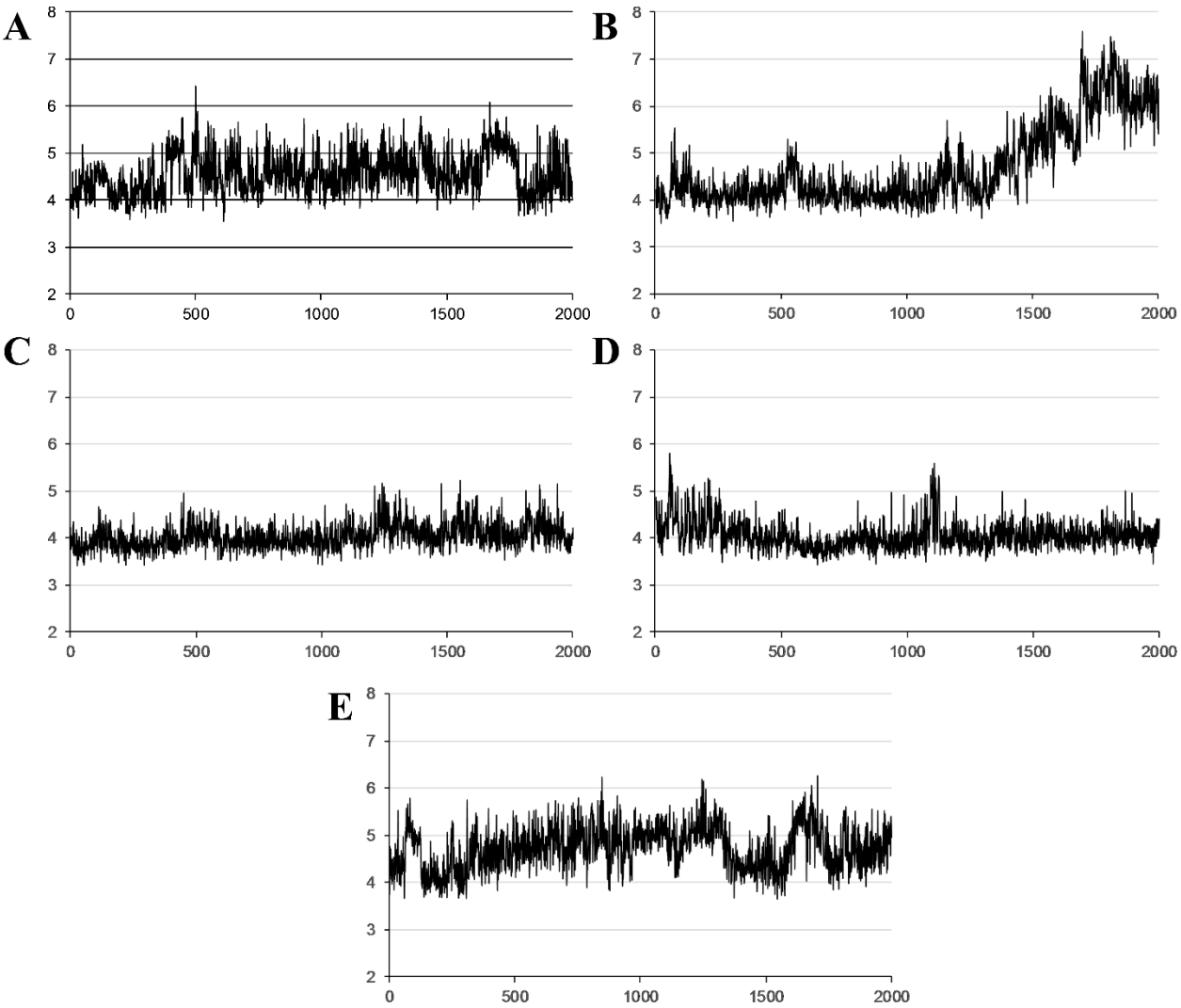

Figure S7: Distances (Å) between atoms described in Table 2 at 2000 snapshots during the 100 ns molecular dynamics simulations.

A: $Ser^{3.35(124)}$-$Glu^{2.53(90)}$

B: $Ser^{3.35(124)}$-$Lys^{2.53(90)}$

C: $Ser^{3.35(124)}$-$Asp^{2.53(90)}$

D: $Ser^{3.35(124)}$-$Arg^{2.53(90)}$

E: $Ser^{3.35(124)}$-$Glu^{2.53(90)}$ of the $Trp^{6.48(280)}$Arg mutant

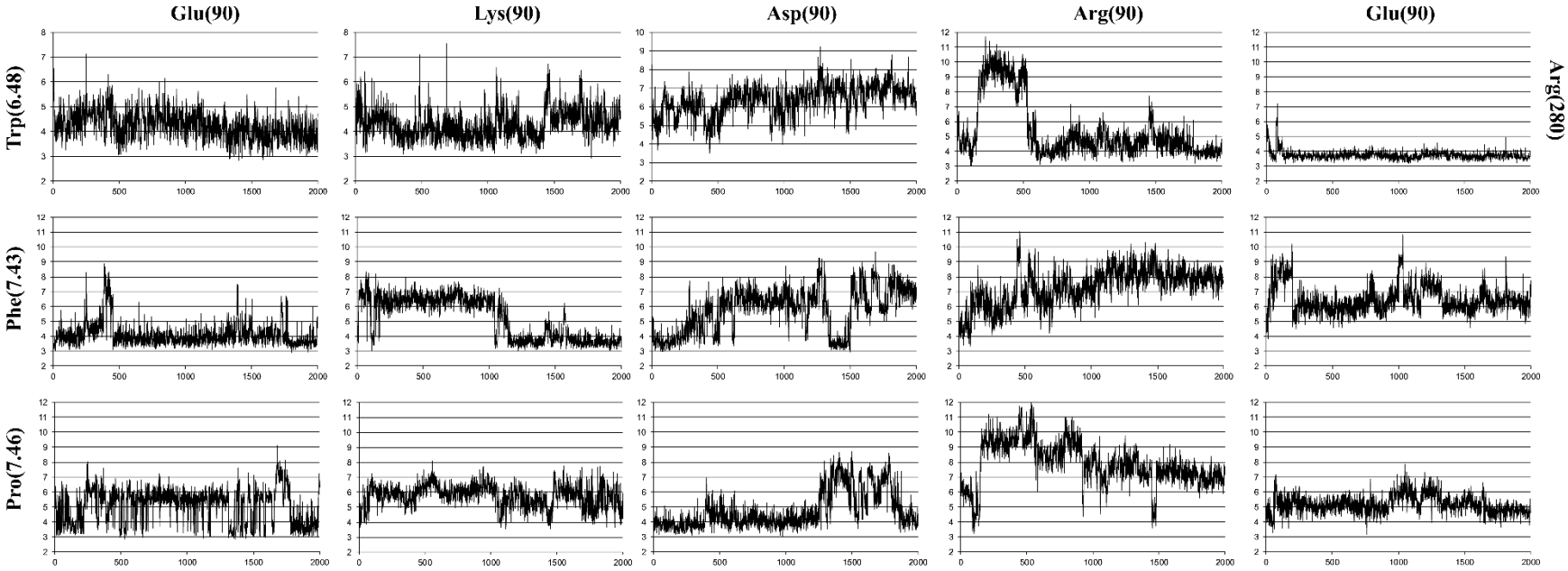

Figure S8: Distances (Å) between atoms described in Table 2 at 2000 snapshots during the 100 ns molecular dynamics simulations.

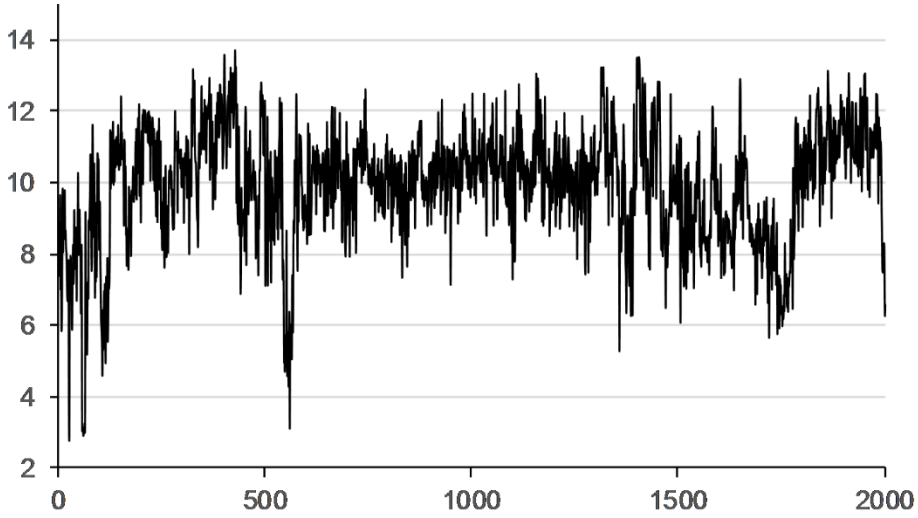

Figure S9: Distance between OE2 of Glu(90) and NZ of Lys(121) at 2000 snapshots during the 100 ns molecular dynamics simulations.

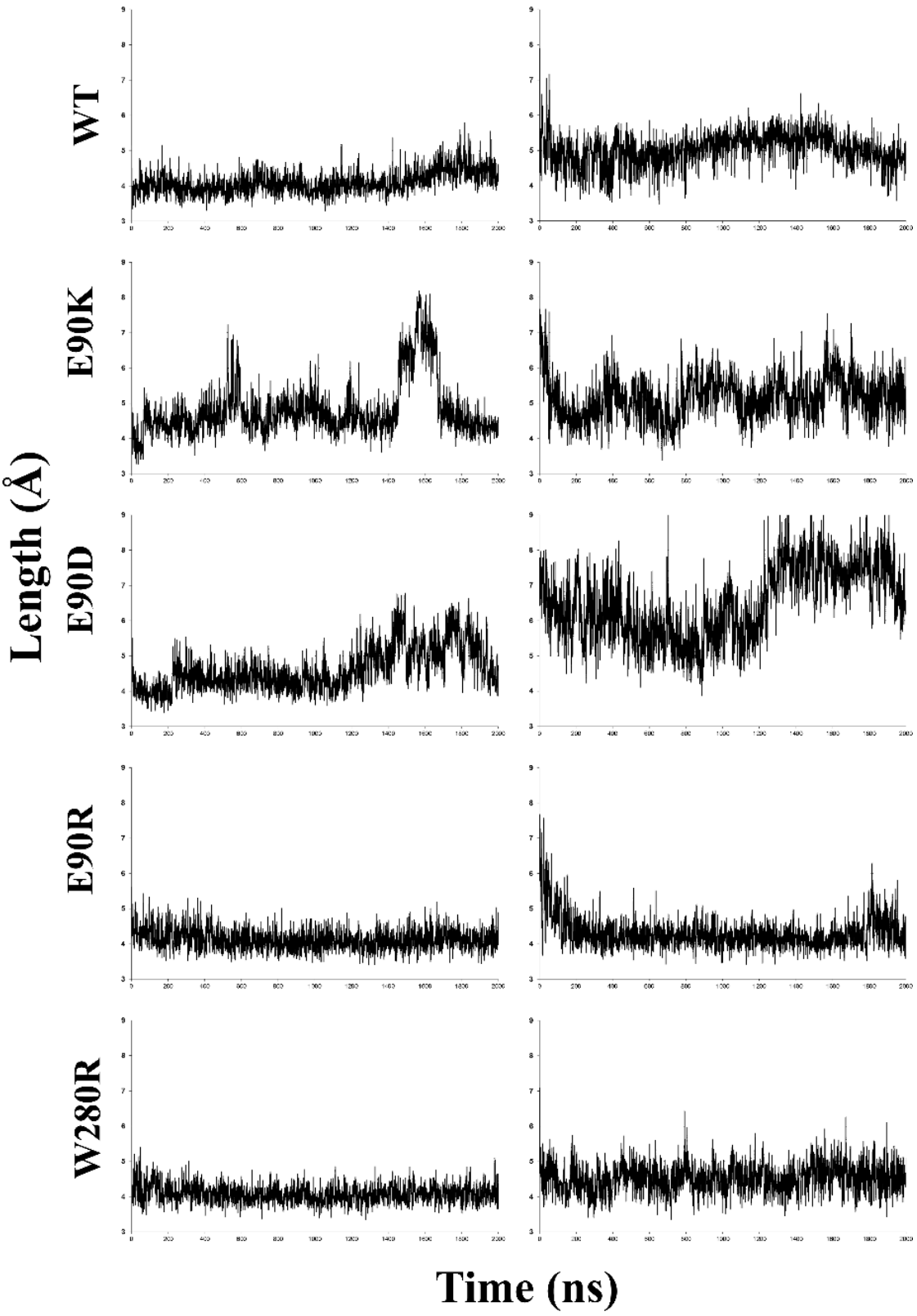
CB.A129 – CG.P223
CG.P223 – CZ.F276
WT
E90K
E90D
E90R
W280R
Length (Å)
Time (ns)

Figure S10: Distances between selected atoms of the core triad residues Ala$^{3.40(129)}$, Pro$^{5.50(223)}$ and Phe$^{6.44(276)}$ at 2000 snapshots during the 100 ns molecular dynamics simulations in wild-type and mutant GnRH receptor models.

References

Berendsen, H.J.C., Postma, J.P.M., van Gunsteren, W.F., DiNola, A., Haak, J.R., 1984. Molecular dynamics with coupling to an external bath. J Chem Phys 81, 3684-3690.

Bussi, G., Donadio, D., Parrinello, M., 2007. Canonical sampling through velocity rescaling. J Chem Phys 126, 014101.

Chien, E.Y., Liu, W., Zhao, Q., Katritch, V., Han, G.W., Hanson, M.A., Shi, L., Newman, A.H., Javitch, J.A., Cherezov, V., Stevens, R.C., 2010. Structure of the human dopamine D3 receptor in complex with a D2/D3 selective antagonist. Science 330, 1091-1095.

Cvicek, V., Goddard, W.A., 3rd, Abrol, R., 2016. Structure-Based Sequence Alignment of the Transmembrane Domains of All Human GPCRs: Phylogenetic, Structural and Functional Implications. PLoS Comput Biol 12, e1004805.

Darden, T., York, D., Pedersen, L., 1993. Particle mesh Ewald: An N· log (N) method for Ewald sums in large systems. J Chem Phys 98, 10089-10092.

Davidson, J.S., Assefa, D., Pawson, A., Davies, P., Hapgood, J., Becker, I., Flanagan, C., Roeske, R., Millar, R., 1997. Irreversible activation of the gonadotropin-releasing hormone receptor by photoaffinity cross-linking: localization of attachment site to Cys residue in N-terminal segment. Biochemistry 36, 12881-12889.

Deupi, X., 2014. Relevance of rhodopsin studies for GPCR activation. Biochim Biophys Acta 1837, 674-682.

Deupi, X., Standfuss, J., 2011. Structural insights into agonist-induced activation of G-protein-coupled receptors. Curr Opin Struct Biol 21, 541-551.

Dore, A.S., Robertson, N., Errey, J.C., Ng, I., Hollenstein, K., Tehan, B., Hurrell, E., Bennett, K., Congreve, M., Magnani, F., Tate, C.G., Weir, M., Marshall, F.H., 2011. Structure of the adenosine A(2A) receptor in complex with ZM241385 and the xanthines XAC and caffeine. Structure 19, 1283-1293.

Edgar, R.C., 2004. MUSCLE: multiple sequence alignment with high accuracy and high throughput. Nucleic Acids Res 32, 1792-1797.

Fenalti, G., Giguere, P.M., Katritch, V., Huang, X.P., Thompson, A.A., Cherezov, V., Roth, B.L., Stevens, R.C., 2014. Molecular control of delta-opioid receptor signalling. Nature 506, 191-196.

Flanagan, C.A., Manilall, A., 2017. Gonadotropin-Releasing Hormone (GnRH) Receptor Structure and GnRH Binding. Front Endocrinol (Lausanne) 8, 274.

Guex, N., Peitsch, M.C., Schwede, T., 2009. Automated comparative protein structure modeling with SWISS-MODEL and Swiss-PdbViewer: a historical perspective. Electrophoresis 30 Suppl 1, S162-173.

Hess, B., 2008. P-LINCS: A Parallel Linear Constraint Solver for Molecular Simulation. J Chem Theory Comput 4, 116-122.

Huang, W., Manglik, A., Venkatakrishnan, A.J., Laeremans, T., Feinberg, E.N., Sanborn, A.L., Kato, H.E., Livingston, K.E., Thorsen, T.S., Kling, R.C., Granier, S., Gmeiner, P., Husbands, S.M., Traynor, J.R., Weis, W.I., Steyaert, J., Dror, R.O., Kobilka, B.K., 2015. Structural insights into m-opioid receptor activation. Nature 524, 315-321.

Isberg, V., Mordalski, S., Munk, C., Rataj, K., Harpsoe, K., Hauser, A.S., Vroling, B., Bojarski, A.J., Vriend, G., Gloriam, D.E., 2017. GPCRdb: an information system for G protein-coupled receptors. Nucleic Acids Res 45, 2936.

Jambeck, J.P., Lyubartsev, A.P., 2012. An Extension and Further Validation of an All-Atomistic Force Field for Biological Membranes. J Chem Theory Comput 8, 2938-2948.

Jambeck, J.P., Lyubartsev, A.P., 2014. Update to the general amber force field for small solutes with an emphasis on free energies of hydration. J Phys Chem B 118, 3793-3804.

Kruse, A.C., Hu, J., Pan, A.C., Arlow, D.H., Rosenbaum, D.M., Rosemond, E., Green, H.F., Liu, T., Chae, P.S., Dror, R.O., Shaw, D.E., Weis, W.I., Wess, J., Kobilka, B.K., 2012. Structure and dynamics of the M3 muscarinic acetylcholine receptor. Nature 482, 552-556.

Kruse, A.C., Ring, A.M., Manglik, A., Hu, J., Hu, K., Eitel, K., Hubner, H., Pardon, E., Valant, C., Sexton, P.M., Christopoulos, A., Felder, C.C., Gmeiner, P., Steyaert, J., Weis, W.I., Garcia, K.C., Wess, J., Kobilka, B.K., 2013. Activation and allosteric modulation of a muscarinic acetylcholine receptor. Nature 504, 101-106.

Lindorff-Larsen, K., Piana, S., Palmo, K., Maragakis, P., Klepeis, J.L., Dror, R.O., Shaw, D.E., 2010. Improved side-chain torsion potentials for the Amber ff99SB protein force field. Proteins 78, 1950-1958.

Lomize, M.A., Pogozheva, I.D., Joo, H., Mosberg, H.I., Lomize, A.L., 2012. OPM database and PPM web server: resources for positioning of proteins in membranes. Nucleic Acids Res 40, D370-376.

Manglik, A., Kruse, A.C., Kobilka, T.S., Thian, F.S., Mathiesen, J.M., Sunahara, R.K., Pardo, L., Weis, W.I., Kobilka, B.K., Granier, S., 2012. Crystal structure of the m-opioid receptor bound to a morphinan antagonist. Nature 485, 321-326.

Miller-Gallacher, J.L., Nehme, R., Warne, T., Edwards, P.C., Schertler, G.F., Leslie, A.G., Tate, C.G., 2014. The 2.1 A resolution structure of cyanopindolol-bound beta1-adrenoceptor identifies an intramembrane Na+ ion that stabilises the ligand-free receptor. PLoS One 9, e92727.

Nickolls, J., Buck, I., Garland, M., Skadron, K., 2008. Scalable parallel programming with CUDA. . Queue 6, 40-53.

Nosé, S., Klein, M., 1983. Constant pressure molecular dynamics for molecular systems. Mol Phys 50, 1055-1076.

Oda, A., Yamaotsu, N., Hirono, S., 2005. New AMBER force field parameters of heme iron for cytochrome P450s determined by quantum chemical calculations of simplified models. J Comput Chem 26, 818-826.

Palczewski, K., Kumasaka, T., Hori, T., Behnke, C.A., Motoshima, H., Fox, B.A., Le Trong, I., Teller, D.C., Okada, T., Stenkamp, R.E., Yamamoto, M., Miyano, M., 2000. Crystal structure of rhodopsin: A G protein-coupled receptor. . Science 289, 739-745.

Park, S.H., Das, B.B., Casagrande, F., Tian, Y., Nothnagel, H.J., Chu, M., Kiefer, H., Maier, K., De Angelis, A.A., Marassi, F.M., Opella, S.J., 2012. Structure of the chemokine receptor CXCR1 in phospholipid bilayers. Nature 491, 779-783.

Pettersen, E.F., Goddard, T.D., Huang, C.C., Couch, G.S., Greenblatt, D.M., Meng, E.C., Ferrin, T.E., 2004. UCSF Chimera--a visualization system for exploratory research and analysis. J Comput Chem 25, 1605-1612.

Pronk, S., Pall, S., Schulz, R., Larsson, P., Bjelkmar, P., Apostolov, R., Shirts, M.R., Smith, J.C., Kasson, P.M., van der Spoel, D., Hess, B., Lindahl, E., 2013. GROMACS 4.5: a high-throughput and highly parallel open source molecular simulation toolkit. Bioinformatics 29, 845-854.

Shimamura, T., Shiroishi, M., Weyand, S., Tsujimoto, H., Winter, G., Katritch, V., Abagyan, R., Cherezov, V., Liu, W., Han, G.W., Kobayashi, T., Stevens, R.C., Iwata, S., 2011. Structure of the human histamine H1 receptor complex with doxepin. Nature 475, 65-70.

Sousa da Silva, A.W., Vranken, W.F., 2012. ACPYPE - AnteChamber PYthon Parser interfacE. BMC Res Notes 5, 367.

Tan, Q., Zhu, Y., Li, J., Chen, Z., Han, G.W., Kufareva, I., Li, T., Ma, L., Fenalti, G., Li, J., Zhang, W., Xie, X., Yang, H., Jiang, H., Cherezov, V., Liu, H., Stevens, R.C., Zhao, Q., Wu, B., 2013. Structure of the CCR5 chemokine receptor-HIV entry inhibitor maraviroc complex. Science 341, 1387-1390.

Thompson, A.A., Liu, W., Chun, E., Katritch, V., Wu, H., Vardy, E., Huang, X.P., Trapella, C., Guerrini, R., Calo, G., Roth, B.L., Cherezov, V., Stevens, R.C., 2012. Structure of the nociceptin/orphanin FQ receptor in complex with a peptide mimetic. Nature 485, 395-399.

Trzaskowski, B., Latek, D., Yuan, S., Ghoshdastider, U., Debinski, A., Filipek, S., 2012. Action of molecular switches in GPCRs-theoretical and experimental studies. Curr Med Chem 19, 1090-1109.

Venkatakrishnan, A.J., Deupi, X., Lebon, G., Heydenreich, F.M., Flock, T., Miljus, T., Balaji, S., Bouvier, M., Veprintsev, D.B., Tate, C.G., Schertler, G.F., Babu, M.M., 2016. Diverse activation pathways in class A GPCRs converge near the G-protein-coupling region. Nature 536, 484-487.

Venkatakrishnan, A.J., Deupi, X., Lebon, G., Tate, C.G., Schertler, G.F., Babu, M.M., 2013. Molecular signatures of G-protein-coupled receptors. Nature 494, 185-194.

Webb, B., Sali, A., 2014. Comparative Protein Structure Modeling Using MODELLER. Curr Protoc Bioinformatics 47, 5 6 1-32.

White, J.F., Noinaj, N., Shibata, Y., Love, J., Kloss, B., Xu, F., Gvozdenovic-Jeremic, J., Shah, P., Shiloach, J., Tate, C.G., Grisshammer, R., 2012. Structure of the agonist-bound neurotensin receptor. Nature 490, 508-513.

Wu, B., Chien, E.Y., Mol, C.D., Fenalti, G., Liu, W., Katritch, V., Abagyan, R., Brooun, A., Wells, P., Bi, F.C., Hamel, D.J., Kuhn, P., Handel, T.M., Cherezov, V., Stevens, R.C., 2010. Structures of the CXCR4 chemokine GPCR with small-molecule and cyclic peptide antagonists. Science 330, 1066-1071.

Wu, H., Wacker, D., Mileni, M., Katritch, V., Han, G.W., Vardy, E., Liu, W., Thompson, A.A., Huang, X.P., Carroll, F.I., Mascarella, S.W., Westkaemper, R.B., Mosier, P.D., Roth, B.L., Cherezov, V., Stevens, R.C., 2012. Structure of the human kappa-opioid receptor in complex with JDTic. Nature 485, 327-332.

Yin, J., Mobarec, J.C., Kolb, P., Rosenbaum, D.M., 2015. Crystal structure of the human OX2 orexin receptor bound to the insomnia drug suvorexant. Nature 519, 247-250.

Zhang, C., Srinivasan, Y., Arlow, D.H., Fung, J.J., Palmer, D., Zheng, Y., Green, H.F., Pandey, A., Dror, R.O., Shaw, D.E., Weis, W.I., Coughlin, S.R., Kobilka, B.K., 2012. High-resolution crystal structure of human protease-activated receptor 1. Nature 492, 387-392.